ELSEVIER

Chemical Engineering Science 59 (2004) 5607–5613

Chemical Engineering Science

www.elsevier.com/locate/ces

Systems analysis and design of dynamically coupled multiscale reactor simulation codes

Effendi Rusli, Timothy O. Drews, Richard D. Braatz*

Department of Chemical and Biomolecular Engineering, University of Illinois at Urbana-Champaign, 114 Roger Adams Laboratory, Box C-3, 600 South Mathews Avenue, Urbana, IL 61801, USA

Received 1 March 2004
Available online 2 November 2004

Abstract

Chemical reacting systems involve phenomena that span several orders of magnitude in time and length scales, from the molecular to the macroscopic. To account for the multiscale character of these processes, many papers have adopted a simulation architecture that employs coupled simulation codes, in which each code simulates the physicochemical phenomena for a different range of length scales in the reacting system. When dynamically coupling codes, it is possible for the codes that solve the individual continuum or non-continuum models to be numerically stable, while the dynamic linkage of the individual codes is numerically unstable. This paper uses control theory to gain insight into these numerical instabilities as well as to design linkage algorithms that modify the dynamic information passed between the individual codes to numerically stabilize their coupling, and to increase the numerical accuracy of the simulation results. The approach is applied to a coupled KMC-FD code for simulating copper electrodeposition in sub-micron trenches.

Keywords: Multiscale systems; Multiscale simulation; Nonlinear systems theory

1. Introduction

Many chemical reaction modeling papers have adopted a multiscale simulation architecture that employs coupled simulation codes, in which each code simulates the physicochemical phenomena for a different range of length scales. Vlachos (1997) linked a surface Monte Carlo model and a fluid-phase continuum reaction/transport model, resulting in a multiscale integration hybrid algorithm to simulate homogeneous/heterogeneous processes. Hansen et al. (2000) incorporated molecular dynamic data into a level set code to simulate the multiscale growth of an aluminum film. A coupled molecular dynamics and Monte Carlo simulation code was used to improve feature-scale simulations of the ionized physical vapor deposition of copper in a trench; the ion sticking probabilities which are location dependent were supplied by a molecular dynamics code to a Monte Carlo code that simulated the trench in-fill (Coronell et al., 2000). Linked codes have been used to simulate metal-oxide semiconductor field effect transistors (MOSFETs) in which a Monte Carlo code computes the electron transport across the MOS which is sent to a finite element (continuum) code that computes the potential and electric field distribution (Hadji et al., 1999). The output of the finite element code was sent back to the Monte Carlo code, and the calculations were repeated iteratively until convergence was obtained. Gobbert et al. (1997) simulated low-pressure chemical vapor deposition by linking a reactor scale code, a feature scale code, and a mesoscale code that mediated the linkage between the other codes. Pricer et al. (2002) linked a coarse-grained kinetic Monte Carlo (KMC) code and a finite difference (FD) code to simulate copper electrodeposition in a variety of surface geometries and studied the additive effects on morphology evolution. Drews et al. (2004) developed a code-coupling algorithm that mediated the boundary conditions dynamically

* Corresponding author. Tel.: +1 217 333 5073; fax: +1 217 333 5052.
E-mail address: braatz@uiuc.edu (R.D. Braatz).

0009-2509/$ - see front matter © 2004 Elsevier Ltd. All rights reserved.
doi:10.1016/j.ces.2004.09.023

passed between the KMC and FD codes, to suppress numerical instabilities and improve the accuracy of the linked simulation.

When dynamically coupling codes, it is possible for the codes that solve the individual continuum or non-continuum models to be numerically stable, while the dynamic coupling of the individual codes is numerically unstable (Raimondeau and Vlachos, 2002). As an illustrative example, consider the multiscale simulation of the copper electrodeposition process (see Fig. 1), which is used in the manufacture of on-chip interconnects for semiconductor devices (Andricacos, 1999). The final product quality is determined by deposit shape and surface morphology, which has a characteristic length scale on the order of nanometers to microns. An accurate description of the deposition process should simultaneously capture the macroscopic transport phenomena of all species in the bulk and the surface phenomena at the working electrode, to resolve key structural properties of copper deposits. The time scales characterizing the deposition process range from a few milliseconds in the electrolytic solution to nanoseconds at the electrode surface.

Fig. 2 shows the information flow between a dynamically coupled FD and KMC simulation code for this process (Drews et al., 2004). The FD code simulates a 2D continuum model for the diffusion and migration of the electrolyte species in the fluid boundary layer, which is described by the material balance for each species and the electrical neutrality condition:

$$\frac{\partial c_i}{\partial t} = \nabla \cdot (D_i \nabla c_i) + z_i F \nabla \cdot (u_i c_i \nabla \Phi), \tag{1}$$

$$\sum_i z_i c_i = 0 \tag{2}$$

with boundary conditions:

$$\text{Top: } c_i = c_i^{\infty}, \quad \Phi = 0,$$
$$\text{Bottom: } N_i = -z_i u_i F c_i \nabla \Phi - D_i \nabla c_i,$$
$$\text{Sides: Periodic,}$$

where c_i, D_i, and z_i are the concentration, the diffusion coefficient, and the ionic charge of species i, respectively, N_i is the species flux at the bottom boundary of the FD domain, F is the Faraday's constant, Φ is the solution potential, and the subscript ∞ denotes the bulk condition.

The KMC code describes the evolution of the deposit shape and surface morphology. On the surface, the cupric ions undergo two charge-transferred reactions:

$$Cu^{2+} + e^- \rightarrow Cu^+, \tag{3}$$

$$Cu^+ + e^- \rightarrow Cu. \tag{4}$$

The cuprous ions are allowed to diffuse freely on the surface to find favorable energy sites before reduction to copper. The simulation domain was coarse-grained to reduce the excessive computational cost. The KMC code simulates

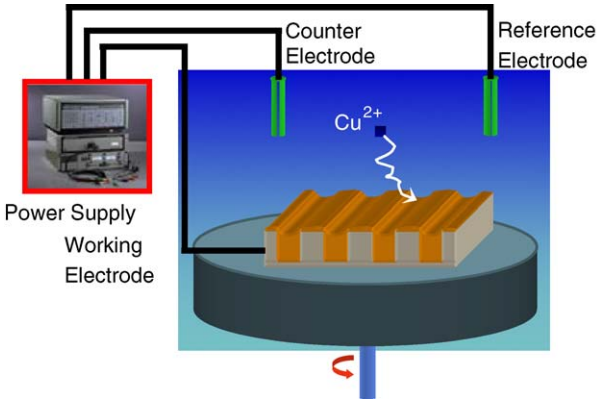

Fig. 1. Electrochemical process for manufacturing on-chip copper interconnects, in which a rotating disk creates a boundary layer above the wafer surface (not drawn to scale).

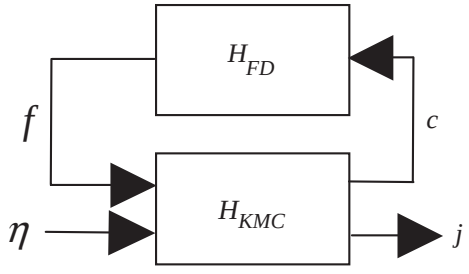

Fig. 2. Dynamic coupled FD–KMC codes used to simulate an electrodeposition process: η is the surface overpotential, and j is the current density.

the electrodeposition phenomena by considering the likelihood of various actions (e.g., adsorption, surface diffusion, reaction) that can occur at each MC time step (see Drews et al., 2004 for details).

At each coupling time instance, the KMC code passes to the FD code the vector of species concentrations, c, at the interface between the FD and KMC spatial domains, and the FD code passes the vector of interface fluxes, f, to the KMC code. The dynamically coupled codes with a coupling time step of 5 ms showed the presence of a numerical instability (see Fig. 3). Choosing a much smaller time step to avoid the numerical instability would make the coupled simulation very computationally expensive without providing enhanced resolution of time scales in the FD code (Drews et al., 2004).

This paper shows how numerically stable code-coupling algorithms can be designed using control theory. First, it is shown how to write a multiscale simulation code in the operator form used in systems theory (shown in Fig. 4). Then nonlinear systems theory is used to make precise statements regarding the well-posedness and numerical stability of dynamically coupled simulation codes. These statements include a constructive procedure for verifying that the dynamic coupling of simulation codes is well-posed and a sufficient condition for the numerical stability of dynamically coupled simulation codes. Then control theory is used to provide

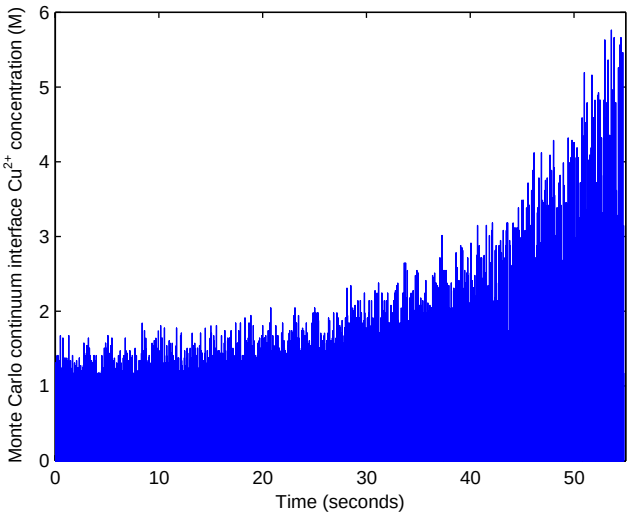

Fig. 3. An interface concentration, c_i, as a function of time, indicating a numerical instability (for details, see Drews et al., 2004).

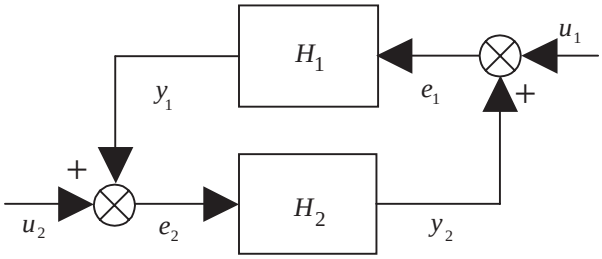

Fig. 4. Coupled codes written in operator form, with $x_t = [x_{1,t}^{\mathrm{T}} \;\; x_{2,t}^{\mathrm{T}}]^{\mathrm{T}}$ for $x = u, e, y$.

guidance for the design of numerically stable algorithms for dynamically coupling simulation codes. The results are illustrated by application to the multiscale simulation of the electrodeposition of copper into a trench.

2. Writing multiscale simulation codes in operator form

Any interconnection of dynamically coupled simulation codes can be written in operator or "block diagram" form. Each block represents an operator between the input and output of each simulation code, and the lines between the blocks represent the transfer of information between simulation codes. This approach is applicable regardless of the time scales, length scales, or numerical algorithm used in each simulation code, including whether each simulation algorithm is deterministic or stochastic. To illustrate these points, consider the dynamic coupling used in the multiscale simulation of the copper electrodeposition problem in Fig. 2. The input–output behavior of the FD code can be written as $f = H_{FD}c$ where the operator H_{FD} is the mapping between the inputs and outputs of the FD code. To write the KMC code in operator form, note that it has an additional input which is implicit in any Monte Carlo code (not shown in Fig. 2), which is the random signal ϑ used to select between possible events in the KMC code. In this particular application, the KMC domain includes events that occur at much smaller time scales than the FD domain, so the KMC code iterates for many thousands of iterations before sending its outputs to the FD code. The input–output behavior of the KMC code can be written as $y_2 = H_{KMC}e_2$, where

$$e_2 = [\, f^{\mathrm{T}} \quad \eta^{\mathrm{T}} \quad \vartheta^{\mathrm{T}} \,]^{\mathrm{T}} \quad \text{and} \quad y_2 = [\, c^{\mathrm{T}} \quad j^{\mathrm{T}} \,]^{\mathrm{T}}.$$

The dynamically coupled code is written in the block diagram form in Fig. 4 by defining

$$H_1 = \begin{bmatrix} H_{FD} & 0 \\ 0 & 0 \end{bmatrix}, \quad H_2 = H_{KMC}, \quad y_1 = [\, f^{\mathrm{T}} \quad 0^{\mathrm{T}} \,]^{\mathrm{T}},$$

$$e_1 = y_2, \quad u_1 = 0, \quad u_2 = [\, 0^{\mathrm{T}} \quad \eta^{\mathrm{T}} \quad \vartheta^{\mathrm{T}} \,]^{\mathrm{T}}, \quad \text{and} \quad e_2 = u_2 + y_1,$$

where 0 is the vector of zeros defined so that the dimensions are consistent.[1]

3. Well-posedness of dynamically coupled simulation codes

As the simulation proceeds, each signal (e.g., e, y, and u in Fig. 4) is a sequence of the form $x = \{x_t, \; t = 0, 1, \ldots\}$, where the index t corresponds to the time instant in which the simulation codes pass information, with x_t belonging to the real vector space of dimension n, denoted by R^n. The first question that arises in the analysis of dynamically coupled simulation codes is whether their interconnection is *well-posed*, that is, whether all signals exist and are unique for any choice of inputs to the coupled codes. For example, the coupling in Fig. 4 is well-posed if the solutions for the sequences $\{e_t\}$ and $\{y_t\}$ exist and are unique for any choice of sequence $\{u_t\}$. A simulation code is *causal* if the value of the output of time t depends only on the values of the inputs up to time t. Any reasonable implementation of a simulation code for a physical system will be causal. A simulation code is *strictly causal* if the output at time t is a function only of the simulation inputs for the times strictly less than t. Strict causality is equivalent to having the simulation output require some time to respond to changes in its input. Any simulation code that uses an explicit solver for time-stepping

[1] A control engineer would refer to the dynamic coupling in Fig. 2 as being *multi-rate*, in that many events occur in the KMC code before the interface concentrations are passed to the FD code. This results in no change in the operator representation in the system, provided that the stochastic signal, ϑ, which changes at the much shorter time interval of the KMC code, is stacked into a vector and the operator H_{KMC} refers to the mapping from the inputs to outputs of the KMC code at each coupling time instance. Then the operator form represents the dynamics at the coupling time instances rather than the KMC time instances. This is a standard approach for addressing multi-rate systems using single-rate analysis, referred to in the literature as *lifting* (Qiu and Tan, 1998).

is strictly causal. Theorem 2 by Vidyasagar (1980) gives a constructive procedure for testing the well-posedness of an arbitrary interconnection of discrete-time nonlinear operators. When applied to an arbitrary interconnection of simulation codes, the sufficient conditions for well-posedness are that: (i) all simulation codes are causal, (ii) some are strictly causal, and (iii) a reduced digraph constructed from this information as well as the pathways of information flow between codes does not contain any cycles or self-loops (see Vidyasagar, 1980 for details). The following lemma specializes the conditions to the interconnection in Fig. 4.

Lemma 1. *The coupled system in Fig.* 4 *is well-posed if both simulation codes H_1 and H_2 are causal and one of the simulation codes is strictly causal.*

4. Numerical stability of dynamically coupled simulation codes

The next question arising in the analysis of dynamically coupled simulation codes is whether the interconnection of simulation codes is numerically stable. For $x \in R^n$, the vector p-norm of $x = [x_1 \;\; x_2 \cdots x_n]^{\mathrm{T}}$ is defined by $\|x\|_p = \left(\sum_{i=1}^{n} |x_i^p|\right)^{1/p}$ for $p \in [1, \infty)$, and $\|x\|_\infty = \max_{1 \leqslant i \leqslant n} |x_i|$. For the infinite sequence $x = \{x_t, \;\; t = 0, 1, \ldots\}$ with $x_t \in R^n$, the l_p-norm of x is defined by $\|x\|_{l_p} = \left(\sum_{t=0}^{\infty} \|x_t\|_p\right)^{1/p}$ for $p \in [1, \infty)$, and $\|x\|_{l_\infty} = \sup_{t=0,1,\ldots} \|x_t\|_\infty$. The space l_p is defined as the set of all discrete signals $x = \{x_t, \;\; t = 0, 1, \ldots\}$ whose l_p-norm is bounded. Now stability can be defined.

Definition 1. [2] Let $x \in l_p$. Then the operator H is *l_p-stable with finite gain* $\gamma(H)$ if there exist non-negative constants $\gamma(H)$ and $\beta(H)$ such that $\|Hx\|_{l_p} \leqslant \gamma(H)\|x\|_{l_p} + \beta(H)$.

For brevity, the term "l_p-stable" is used in this paper to refer to "l_p-stable with finite gain". The integer p in the above definitions is selected as a matter of convenience. Checking whether a simulation code is l_∞-stable is especially easy to test, since all this means is that the simulation outputs are bounded for bounded simulation inputs. Another relatively easy check is whether a simulation code is l_2-stable, as this just means that the simulation outputs have bounded energy for all simulation inputs with bounded energy, where this notion of energy is a generalization of energy as taught in thermodynamics.

For brevity, the focus here is on the coupling of two simulation codes that pass updated boundary conditions at a shared interface between the physical domains simulated by the two codes. Similar results hold when more than two simulation codes are dynamically coupled, including when there is spatial overlap between domains. The following is one of the classic results of nonlinear stability theory.

[2] This definition of l_p-stability is more general than that most commonly used in control theory (e.g., Zhou et al., 1996), which assumes that $\beta(H) = 0$. The more general definition is needed for the application of nonlinear systems theory to simulation codes because most simulation codes do not produce a zero-norm output for a zero-norm input. For example, for the FD code in Fig. 2, a zero interface concentration does not imply a zero interface flux.

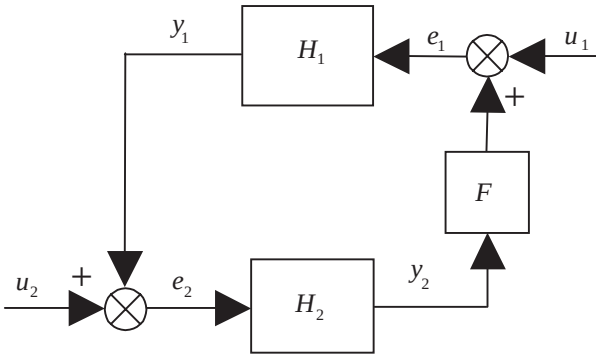

Fig. 5. Interconnected system that incorporates the code-coupling filter F.

Theorem 1 (*Small Gain Theorem*). *Consider the interconnected system in Fig.* 4. *Suppose that the operators H_1 and H_2 are causal and l_p-stable*: $\|H_1 x\|_{l_p} \leqslant \gamma(H_1)\|x\|_{l_p} + \beta(H_1)$, $\|H_2 x\|_{l_p} \leqslant \gamma(H_2)\|x\|_{l_p} + \beta(H_2)$, *where* $\gamma(H_1)$, $\gamma(H_2)$, $\beta(H_1)$, $\beta(H_2) \geqslant 0$ *and* $p \in [1, \infty]$. *Then the system in Fig.* 4 *is l_p-stable if* $\gamma(H_1)\gamma(H_2) < 1$.

Theorem 1 provides a sufficient condition for the numerical stability of two dynamically coupled simulation codes. As an example application, for the coupled KMC–FD codes described in Fig. 2, both simulation codes are causal since the codes were constructed from first-principles models, and l_∞-stable since the codes produce bounded outputs for bounded inputs (each individual code is numerically stable and the physical systems do not have variables that "blow up"). Then Theorem 1 gives that a sufficient condition for numerical stability is that $\gamma(H_{FD})\gamma(H_{KMC}) < 1$, which is the product of the gains for the individual simulation codes.

As the practical application of this result, it is well-known that introducing a filter can reduce the gain of a system, that is, a filter F can be designed such that $\gamma(FH_i) < \gamma(H_i)$. This suggests that inserting a filter into Fig. 4, to give Fig. 5, may numerically stabilize a dynamically coupled simulation code. This is precisely the approach taken by Drews et al. (2004) to numerically stabilize the coupled FD–KMC simulation codes in Fig. 2. The next section applies control theory to guide the design of this filter, F, to numerically stabilize the dynamically coupling of two simulation codes, while improving their accuracy in simulating the true dynamics of the multiscale system.

5. Design of a numerically stable code-coupling algorithm

Although the overall approach taken here applies to general interconnections of coupled simulation codes, for

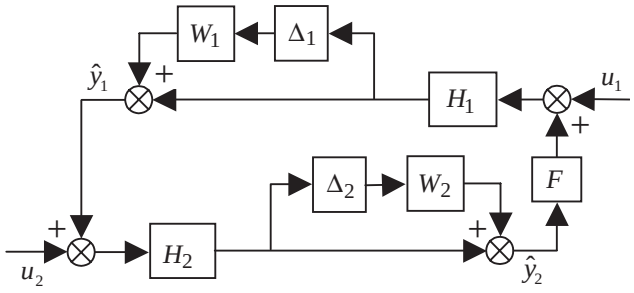

Fig. 6. Interconnected systems with perturbations used in the filter analysis.

brevity and illustration purposes, this paper will focus on the application to the coupled codes in Figs. 2 and 4. In this section H_1 and H_2 in Fig. 4 refer to the operators describing the real physical systems, with $H_{1c} = (I + W_1\Delta_1)H_1$ and $H_{2c} = (I + W_2\Delta_2)H_2$ referring to the operators describing the corresponding simulation codes which provide numerical approximations of the input–output behavior of the real physical systems. As is standard in robust control theory (Zhou et al., 1996), Δ_i are unitary norm-bounded perturbation operators with weights W_i selected to be minimum phase and stable linear time invariant operators that quantify the approximation error between the real physical systems and the corresponding simulation codes. The weights W_i have a low response at low frequencies (which means that the simulation codes accurately capture long time behavior) and high response at high frequencies (where the simulation codes are expected to be less accurate). The example demonstrates how these weights can be designed to incorporate the error contribution from the time delay in the information passing between the codes.

The following assumptions are made: (i) the operators H_1, H_2, F, W_1, W_2, Δ_1, and Δ_2, are l_p-stable, (ii) the interconnection in Fig. 4 is well-posed and l_p-stable. Assumption (ii) implies that the variables in the real physical system are well-posed and do not "blow up" for bounded inputs. As is typical when studying robust control problems, linear systems theory will be used to design a compensator (in this case, the filter F) based on linearizations of the nonlinear operators, so henceforth H_1 and H_2 refer to the linearized operators.

With the definitions $y = [y_1^{\mathrm{T}}\ y_2^{\mathrm{T}}]^{\mathrm{T}}$ and $u = [u_1^{\mathrm{T}}\ u_2^{\mathrm{T}}]^{\mathrm{T}}$ in Fig. 4, the mapping from u to y, $y = N_T u$, is given by

$$N_T = \begin{bmatrix} (I - H_1H_2)^{-1}H_1 & (I - H_1H_2)^{-1}H_1H_2 \\ H_2(I - H_1H_2)^{-1}H_1 & H_2(I - H_1H_2)^{-1} \end{bmatrix}, \quad (5)$$

where I is the identity operator of appropriate dimensions. Assumption (ii) implies that the operator N_T is l_p-stable. It is assumed that the coupled simulation codes are numerically unstable, so that the interconnection in Fig. 4 is not l_p-stable when H_1 and H_2 are replaced by H_{1c} and H_{2c}. The goal of the filter F in Fig. 6 is to numerically stabilize the coupled codes, which means to stabilize the interconnection in Fig. 6 for all allowed perturbations Δ_i, while maintaining consistency between the real physical system and the coupled simulation codes. In general a filter could be located at the output of each simulation code; here the filter was located only at the output of the KMC code, because the KMC code is not as accurate as the FD code in describing the behavior of the real physical system, and that such a filter location has the additional advantage of directly suppressing the effects of KMC simulation noise on the dynamics of the coupled codes.

Theorem 2. *Consider the block diagram in Fig.* 6 *under Assumptions* (i)–(ii). *Let* $d_1, d_2 \in R^1$ *be positive. Suppose that there exists a constant* $k > 0$ *such that the following conditions hold*:

(a) *the interconnection in Fig.* 4 *is well-posed and* l_p*-stable*,
(b) *the interconnection in Fig.* 5 *is well-posed and* l_p*-stable*,
(c) $\max\{\gamma(W_1), \gamma(FW_2)\} < k$,
(d) $\inf_{d_1,d_2>0} \gamma(DN_1D^{-1}) < 1/k$, *where* $D = \begin{bmatrix} d_1 I & \\ & d_2 I \end{bmatrix}$ *and*

$$N_1 = \begin{bmatrix} (I - H_1FH_2)^{-1}H_1FH_2 & (I - H_1FH_2)^{-1}H_1 \\ H_2(I - H_1FH_2)^{-1} & H_2(I - H_1FH_2)^{-1}H_1 \end{bmatrix}. \quad (6)$$

Then the interconnection in Fig. 6 *is* l_p*-stable for all unitary norm-bounded perturbations,* $\Delta_i \in \{\Delta\colon\ \gamma(\Delta) \leqslant 1, \beta(\Delta) = 0\}$.

Proof. The input–output mapping in Fig. 6 can be written as

$$\hat{y} = (I - N_1N_w\Delta)^{-1}N_2u, \quad (7)$$

where

$$N_w = \begin{bmatrix} W_1 & \\ & FW_2 \end{bmatrix}, \quad \Delta = \begin{bmatrix} \Delta_1 & \\ & \Delta_2 \end{bmatrix},$$
$$N_2 = \begin{bmatrix} (I - H_1FH_2)^{-1}H_1 & (I - H_1FH_2)^{-1}H_1FH_2 \\ H_2(I - H_1FH_2)^{-1}H_1 & H_2(I - H_1FH_2)^{-1} \end{bmatrix}. \quad (8)$$

Condition (b) implies that N_1 and N_2 are l_p-stable. Hence the interconnection in Fig. 6 is l_p-stable if and only if

$$\begin{aligned}
&(I - N_1N_w\Delta)^{-1} \text{ is } l_p\text{-stable} \\
&\quad \leftrightarrow D^{-1}(I - DN_1D^{-1}DN_w\Delta D^{-1})^{-1}D \text{ is } l_p\text{-stable} \\
&\quad \leftrightarrow (I - DN_1D^{-1}DN_w\Delta D^{-1})^{-1} \text{ is } l_p\text{-stable} \\
&\quad \leftarrow \gamma(DN_1D^{-1})\gamma(DN_w\Delta D^{-1}) < 1 \\
&\quad \leftrightarrow \gamma(DN_1D^{-1})\gamma(N_wD\Delta D^{-1}) < 1 \\
&\quad \leftarrow \gamma(DN_1D^{-1})\gamma(N_w)\gamma(D\Delta D^{-1}) < 1 \\
&\quad \leftarrow \gamma(D\Delta D^{-1}) < 1, \gamma(N_w) < k, \text{ and} \\
&\qquad \gamma(DN_1D^{-1}) < 1/k \\
&\quad \leftarrow \gamma(\Delta) < 1, \gamma(W_1) < k, \gamma(FW_2) < k, \text{ and} \\
&\qquad \gamma(DN_1D^{-1}) < 1/k,
\end{aligned}$$

where the latter part of the second relation follows from Theorem 1. □

Recall that condition (a) in Theorem 2 just states that the interconnection of the real physical systems is well-posed and does not have signals that "blow up" with time. As discussed earlier, condition (a) is a mild condition. Condition (b) states that the interconnection of the real physical systems is well-posed and does not have signals that "blow up" with time when a filter is introduced into the system. For the design reasons discussed below, the filter F is selected to be low pass. If the filter is selected to be m first-order linear time-invariant systems in series, then a physical process with this transfer function is m equivalent well-mixed systems in series. That is, the introduction of this filter F into the physical system would introduce a lag into the dynamics of the interconnected system, which for a physical system is not likely to introduce instability. That is, condition (b) is very likely to hold if condition (a) holds. The next lemma shows that condition (b) in Theorem 2 is obtained "for free" when l_p-stability of the interconnection in Fig. 4 can be proven using the small gain theorem (Theorem 1).

Lemma 2. *Suppose that the interconnection in Fig.* 4 *is well-posed and l_p-stable, that the operators H_1 and H_2 are l_p-stable and causal, the filter F is strictly causal, and that $\gamma(F) \leqslant 1$ and $\gamma(H_2H_1) < 1$. Then the interconnection in Fig.* 5 *is well-posed and l_p-stable.*

Proof. The strict causality of F with Lemma 1 implies that the interconnection in Fig. 5 is well-posed. The operator N_2 in Eq. (8) can be written in terms of $(I - FH_2H_1)^{-1}$ or $(I - H_2H_1F)^{-1}$ using the identities $(I - H_1FH_2)^{-1}H_1 = H_1(I - FH_2H_1)^{-1}$ and $(I - H_2H_1F)^{-1}H_2 = H_2(I - H_1FH_2)^{-1}$. With Theorem 1, this implies that the interconnection in Fig. 5 is l_p-stable if $\gamma(F)\gamma(H_2H_1) < 1$. □

Condition (c) of Theorem 2 quantifies the differences in input–output behavior of the real physical systems and the simulation codes, and motivates the positioning of the filter F at the output of the KMC code. The weights W_i should be selected to be high pass for most simulation codes, since the input–output behavior of a simulation code deviates from that of the real physical system for the shortest time scales. This behavior, which occurs for nearly any model for a real physical system, is referred to as *unmodeled dynamics* in the controls literature. In the coupled KMC–FD code, the uncertainties associated with the KMC code were rather large, so the filter F is positioned so that it can reduce the effects of these uncertainties on the coupled system. The filter F should be tuned based on condition (c), since F has a more direct effect on the gain in condition (c) than the gain in condition (d). Condition (c) indicates that the filter F should be designed to suppress the effects of the uncertainties of the KMC code, which are quantified by the high pass weight W_2. Since both W_2 and F are linear time invariant, even when the operators H_i are nonlinear, the filter F can be designed by plotting FW_2 in the frequency domain, and selecting the dynamics of F to roll off at the frequencies where the uncertainties in the KMC code are considered likely to be significant (where $|W_2(e^{-j\omega})|$ is large), so that $\gamma(FW_2)$ is significantly less than $\gamma(W_2)$.

Algorithms exist for solving the optimization in condition (d) (e.g., see Zhou et al., 1996). Conditions (c) and (d) can be used to show that the simulation codes are numerically stabilized if sufficient filtering is performed. The next result considers tuning F for numerical accuracy.

Theorem 3. *Define M by $\hat{y} - y = Mu$ and $\gamma_2(M)$ as the gain of M for $p = 2$, where y is the vector of outputs of the real physical system defined in Fig.* 4 *and $\hat{y}$ is the vector of outputs defined in Fig.* 6. *Then $\gamma_2(M) < k$ if the conditions of Theorem* 2 *are satisfied with $p = 2$ and*

$$\inf_{d_1,d_2\neq 0} \gamma_2\left(\begin{bmatrix} d_1 I & \\ & d_2 I \end{bmatrix}\begin{bmatrix} N_1N_w & N_2 \\ k^{-1}N_1N_w & k^{-1}(N_2 - N_T) \end{bmatrix} \times \begin{bmatrix} d_1^{-1}I & \\ & d_2^{-1}I \end{bmatrix}\right) < 1. \tag{9}$$

Proof. With $M = (I - N_1N_w\Delta)^{-1}N_2 - N_T$, block diagram manipulation and robust performance theory (Zhou et al., 1996) gives the condition in (9). □

When the perturbations are negligible ($N_w \approx 0$), then Eq. (9) simplifies to

$$\gamma_2(N_2 - N_T) < k. \tag{10}$$

Hence a filter designed to minimize the error $\hat{y} - y$ should minimize the left-hand side of Eq. (10). Consequently, a filter designed to barely achieve numerical stability of the coupled codes does not yield simulation results that are most consistent with the real physical system.

As the operator N_T reduces to N_2 when $F = I$, the code-coupling filter should be designed to equal the identity operator except for frequencies where the weight W_2 is large.

For the electrochemical system, the weight W_2 designed to cover the $\delta t = 5$ ms temporal mismatch between the codes is plotted in Fig. 7.[3] Fig. 8 shows the interface concentration of copper ions as a function of time after insertion of the first-order filter between the KMC and FD codes designed according to the above design rules (low-pass filter with steady-state gain of one that rolls off for frequencies where the weight W_2 is large). Fig. 8 indicates that the filter successfully suppresses the numerical stability that arose when directly coupling the FD and KMC codes.

[3] Details on the design of a weight to bound time delay variation are given on pp. 119–120 of Morari and Zafiriou (1989).

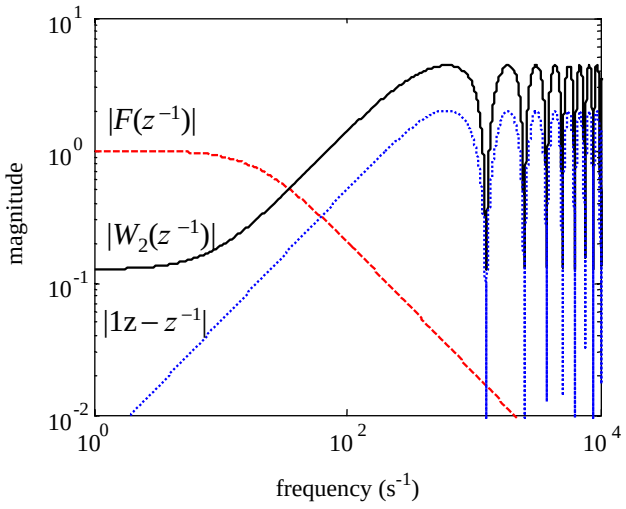

Fig. 7. Frequency domain representation for the multiplicative uncertainty weight $W_2(z^{-1}) = -2.0857z^{-1}/(1 - 0.1218z^{-1} + 2.5)$ for the KMC simulation, the uncertainty $|1 - z^{-1}|$ due to temporal coupling mismatch, and the stabilizing filter $F(z^{-1}) = 0.1/(1 - 0.9z^{-1})$, where $z = e^{j\omega\delta t}$ and $\omega \in [0, 2\pi/\delta t)$.

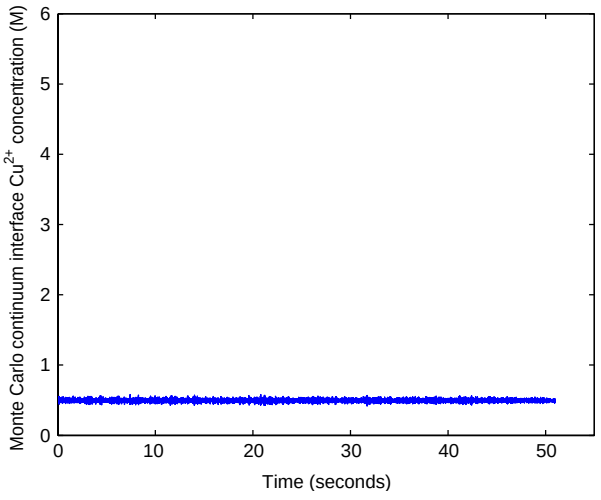

Fig. 8. The interface concentration of copper ions as a function of time has been stabilized by inserting a filter between the KMC and FD codes.

6. Conclusions

This paper showed how control theory can be used to design numerical algorithms for coupling simulation codes. Nonlinear systems theory provided a constructive procedure for testing whether an arbitrary interconnection of simulation codes is well-posed, and a sufficient condition for the numerical stability of dynamically coupled simulation codes. Linear systems theory provided specific design requirements for a code-coupling filter for a pair of dynamically coupled FD-KMC codes for simulating a multiscale copper electrodeposition process. Systems theory elucidated the trade-off in filter design between providing numerical stability and numerical accuracy.

Acknowledgements

This material is based upon work supported by the National Science Foundation under grant numbers CTS-0135621, CISE-9619019, and PACI NRAC MCA-01S022. Any opinions, findings, and conclusions or recommendations expressed in this paper are those of the authors and do not necessarily reflect the views of the National Science Foundation.

References

Andricacos, P.C., 1999. Copper on-chip interconnections—a breakthrough in electrodeposition to make better chips. The Electrochemical Society Interface 8, 32.

Coronell, D.G., Hansen, D.E., Voter, A.F., Liu, C., Liu, X., Kress, J.D., 2000. Molecular dynamics-based ion-surface interaction modes for ionized physical vapor deposition feature scale simulations. Applied Physics Letters 73, 3860.

Drews, T.O., Webb, E.G., Ma, D.L., Alameda, J., Braatz, R.D., Alkire, R.C., 2004. Coupled mesoscale-continuum simulations of copper electrodeposition in a trench. A.I.Ch.E. Journal 50, 226.

Gobbert, M.K., Merchant, T.P., Borucki, L.J., Cale, T.S., 1997. A multiscale simulator for low pressure chemical vapor deposition. Journal of the Electrochemical Society 144, 3945.

Hadji, D., Marechal, Y., Zimmerman, J., 1999. Finite element and Monte Carlo simulation of submicrometer silicon n-MOSFET's. IEEE Transactions on Magnetics 35, 1809.

Hansen, U., Rodgers, S., Jensen, K.F., 2000. Modeling of metal thin film growth: linking angstrom-scale molecular dynamics results to micron-scale film topographies. Physical Reviews B 62, 2869.

Morari, M., Zafiriou, E., 1989. Robust Process Control, Prentice-Hall, Englewood Cliffs, NJ.

Pricer, T.J., Kushner, M.J., Alkire, R.C., 2002. Monte Carlo simulation of the electrodeposition of copper—Parts I and II. Journal of the Electrochemical Society 149, C396.

Qiu, L., Tan, K., 1998. Direct state space solution of multirate sampled-data H-2 optimal control. Automatica 34, 1431.

Raimondeau, S., Vlachos, D.G., 2002. Recent developments on multiscale, hierarchical modeling of chemical reactors. Chemical Engineering Journal 90, 3.

Vidyasagar, M., 1980. On the well-posedness of large-scale interconnected systems. IEEE Transactions on Automatic Control AC-25, 413.

Vlachos, D.G., 1997. Multiscale integration hybrid algorithms for homogeneous–heterogeneous reactors. A.I.Ch.E. Journal 43, 3031.

Zhou, K., Doyle, J.C., Glover, K., 1996. Robust and Optimal Control, Prentice-Hall, Upper Saddle River, NJ.